

Measurements of Hole Shape on Carbon-Carbon Composite Grid after 20,000-hour Endurance Test

IEPC-2007-090

*Presented at the 30th International Electric Propulsion Conference, Florence, Italy
September 17-20, 2007*

Miyuki USUI*

University of Tokyo, Hongo, Tokyo, 113-8656, Japan

Hitoshi KUNINAKA†

Japan Aerospace Exploration Agency, Sagamihara, Kanagawa, 229-8510, Japan

Abstract: In the flight model of the ion engine, the endure test of tens of thousands of hour class is done in real time for the durability assessment. For example, the ion engine $\mu 10$ in *Hayabusa* program was devoted to the 20,000-hour endure test in twice, so that their endurance was qualified. However, the long duration test like *Hayabusa* program is not realistic any longer, because of improvement of durability and requirement of long life. Therefore, the following endurance qualification method is proposed; the combination of the endure test in several thousand hours and the numerical estimation for the service life assessment. Then, we measurement the hole shape of the electrostatic grid of prototype of the ion engine $\mu 10$ after 20,000 hour endurance test. As a result, abrasion of screen grid hole is little. In the other hand, accelerator grid hole and decelerator grid hole are large before endurance test. In particular, decelerator grid hole looks like pot type (rim of downstream side is flare.).

I. Introduction

The high specific impulse that is feature of the ion engines makes good use of operating for a long time such as an orbital transfer mission. A lot of the ion engines in fixed satellites and explorer have already proven the operation of 10,000 hours. The most important factor of life limiting in ion engine is ion accelerating electrode, named grid because of sputter erosion of grid material by ion impingement. Even if the ions are properly focused when they are passing through a grid hole of an accelerator grid, charge-exchange ions are produced as a result of the interaction between slow neutral atoms leaking from the screen grid and the fast ion beam. The created slow ions are attracted to the negatively biased accelerator grid and steadily erode the surface of the accelerator grid. If the erosion advances to a severe level, beyond which electron backstreaming of electrons from the neutralizer occurs due to accelerator aperture enlargement from sputter erosion, the ion extraction and acceleration end of life. As for the wear of the other grid, the decelerator grid does not suffer from such wear provide the beam is focused correctly. In contrast, the screen grid also receives ion impingement from the plasma inside the discharge chamber. The described grid erosion mechanisms are considered the most critical and inevitable life-limiting factor, excluding random events that could lead to a grid-to-grid short.¹

As a best combination of mechanical properties as well as low sputter yield, molybdenum is usually used for the ion optics. However, even molybdenum suffers from severe erosion, limiting the life time of the accelerator grid. One way to overcome this life-limiting issue is to employ a material with higher resistance to ion sputter damage,

* Graduate student, Department of Aeronautics and Astronautics, E-mail: usui@ep.isas.jaxa.jp

† Professor, Department of Space Transportation Engineering, E-mail: kuninaka@isas.jaxa.jp

such as carbon. For this purpose, we employed a carbon-carbon (C/C) composite material, in which fragile graphite is reinforced with carbon fibers to survive a vibrational environment of a spacecraft launch. The C/C composite was intensively studied from the early 1990s, especially at the Boeing Company and the Jet Propulsion Laboratory as are placement for molybdenum grid. After a successful demonstration of the first C/C ion optics,² C/C's lower sputter yield was confirmed.³ However, its weak mechanical properties and difficulty in fabrication prevented its practical application, and accordingly drove researchers toward pursuing a number of fabrication techniques that improved its structural strength.⁴⁻⁷ A difficulty of the C/C grid originates in its contradicted requirement: Strong mechanical properties are required in a thin plate with many holes in a large open area fraction. In spite of such difficulties, ESA and NASA continue the development of the C/C grids through contracts with commercial companies^{8, 9} because the C/C composite is considered as a next-generation grid material for high-performance ion engines. Until now, as far as we know, no C/C grid system was qualified for a satellite application, which demands such qualification processes as a long-term life test, and a vibrational test simulating the space craft launch condition.

However, for the improvement of grid material durability that described in the above-mentioned and the requirement of long-time mission using ion engine, real-time endurance test is no longer realistic. Instead, numerical lifetime prediction and real-time is necessary (if we need the endurance test, it is operated for several thousand of hour class.).

Then we measure the hole shape of the electrostatic grids that had actually done 20,000 hour endurance test. These grids were parts of prototype model (PM) of microwave discharge ion engine which is installed in the Japanese space probe named MUSES-C "Hayabusa", executed the scientific observation¹⁰ and the touchdown on the asteroid surface and aims to bring back samples from the asteroid. This measurement result will contribute the development of the numerical tool for the service life assessment.

II. Grid Optics Description

Flat, circular grids, of 10 and 12 cm diam, were fabricated from a 30-cm-square C/C panel. C/C composite is a structure consisting of fibrous carbon substrates in a carbonaceous matrix. As a carbon fiber, a pitch-based carbon fiber felt was selected, which consists of tangled continuous filaments of about 10 μ m in diameter. To get additional strength and mechanical stability, the carbon matrix is deposited on the pitch-based fibers by a chemical vapor infiltration (CVI) technique.¹⁰ This technique densifies the composite panel at temperatures beyond 1000 K and minimizes the number and the size of pores between the fibers. Resulting C/C panel properties for PM summarized in Table 1 (also see Ref.11). The material strength of C/C is inferior to that of molybdenum and the state-of-the art C/C panel. This is because the felt-type C/C does not consist of woven long carbon fibers that reinforce the C/C panel. However, the tangled microcarbon fiber structures of the felt carbon create an isotropic composite, which can be easily machined into a desired shape with an acceptable tolerance and surface roughness. Even after the drilling, part of these microcarbon structures remains between the holes, sustaining the overall structure of the C/C plate. Hence, after the C/C composite is shaped into a thin plate, a precise mechanical drilling creates a grid hole. Fabricated grid dimensions are summarized in Table 2. Note the very clean surface and that the straight hole profile

Table 1. Material property of C/C composite sample

Property	PM	Typical Mo (Ref. 16)
Density, g/cm ³	1.6	10.2
Tensile strength, MPa	87	490
Flexural strength, MPa	130	N/A
Tensile modulus, GPa	25	327
Flexural modulus, GPa	21	327
Thermal expansion, /K	2 \times 10 ⁻⁵	5 \times 20 ⁻⁵

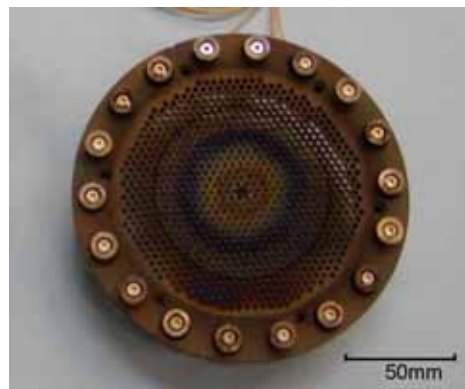


Figure1. Grid design; three grids mounted on a ring

without delamination, cracks or fiber pullout is confirmed.

the rigid mount system shown in Fig. 1 was designed. The C/C grid plates are mounted via ceramic spacers to an aluminum ring, and the grids are separated from each other by the spacers. Their gaps are precisely adjusted when they are torqued to the ring. With this fastened grid attachment, the grid increases its strength and the grid-to-grid gap can be controlled to ± 0.04 mm accuracy. The mechanical test result of this grid mount was good.

III. Endurance Test of Prototype Model

The microwave discharge ion engine was located in main chamber of 2 m in diam and 5 m in length, which is evacuated by four cryogenic pumps, maintaining an order of 10^{-6} torr for the xenon mass flow rate of 2 sccm.

The PM phase (second time 18,000 hours) endurance test began from April 2000. In this time not only the accelerator grid but also the whole ITR is dedicated to the 18,000 hours endurance test again. The testing conditions for PM endurance test, the minimum requirement of the screen current for the initial 9,000 hours and that for the 18,000 hours are different because they are the orbit interface minimum requirements to and from the asteroid. As the history exhibits, there has been no suspension of the endurance test except the momentary interruption of PM phase system test using PM ITR as the actual load and the thrust performance evaluation of temperature effects on the PM grids. The second time 18,000 hours was achieved October 2002 (Fig2 and 3). Ultimately, PM ITR was operated for 20,000 hours. Operational condition for the endurance test was summarized in Table 3.

Table 3. Test Conditions

Property	PM
Voltage, V	
Screen	1500
Accelerator	-350
Decelerator	GND
Bream current, mA	135
Accelerator current, mA	0.5
Microwave power, W	
Ion source	<35
Neutralizer	<8
Xe flow rate, sccm	
Ion source	2.35
Neutralizer	0.5
Vacuum, torr	-10^{-5}

Table 2. Ion optics geometry

Property	PM
Objective	Endurance test
C/C fiber	Pitch-based felt
Grid shape	Circular, flat
Beam diameter, mm	105
Hole quantity	855
Hole axial profile	Straight
Open area function, %	
Screen	67
Accelerator	24
Decelerator	47
Hole diameter, mm	
Screen	3.0
Accelerator	1.8
Decelerator	2.5
Thickness, mm	
Screen	1
Accelerator	1
Decelerator	1
Gap	
Screen to Accelerator	0.32
Accelerator to Decelerator	0.5

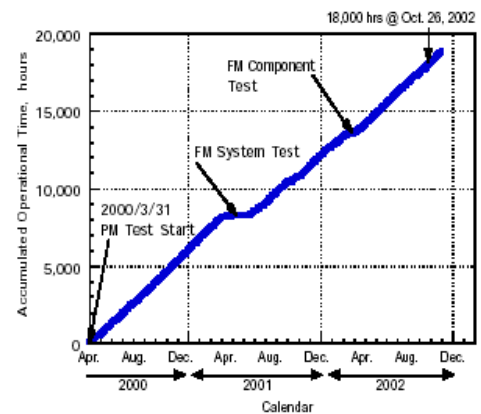


Figure 2. PM Accumulated operation time

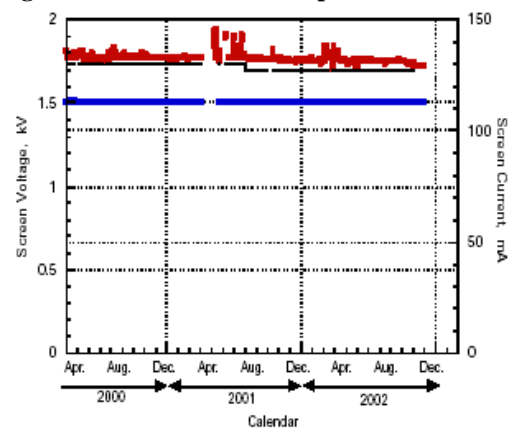


Figure 3. PM-phase endure test history screen voltage and current

IV. Measurement and Result

A. 3 Dimensional Shape Measurements

Figure 4 shows digital microscope used by measurement of hole shape. It can measure shape three dimensional because the plane image taken a picture of by various focal lengths is synthesized in the focus. As a result the no contact measurement became possible. To obtain shape on sidewall of the grid, this microscope is inclined to 45 degrees and we measured grid holes from 12 directions every 30 degrees of downstream side and upstream side.

Basing on this measurement result, the section shape characteristic of the grid hole and the radius characteristic to the surroundings direction angled.

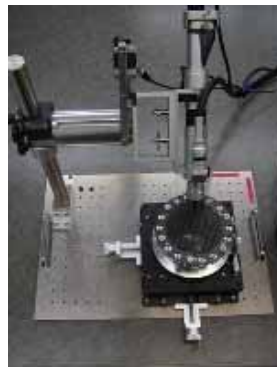


Figure 4. Digital microscope Figure 5 PM ion engine

B. Observation of hole shape

We observed the entire appearance of grids before measurement of hole. Figure 5 shows PM ion engine after 20,000-hour endurance test. There is symmetry in the entire grid after endurance test. Therefore, it is important that holes on center axis “x” or “r” row in grid, which is shown Fig 6, observe and measure. The r row consists of 31 holes. The most outer hole on the r row is named r1 and other holes are also. So, r16 is center hole. Then, we observe r2, r7, r11 and r16 on the screen grid, the accelerator grid and the decelerator grid of downstream side and upstream side.

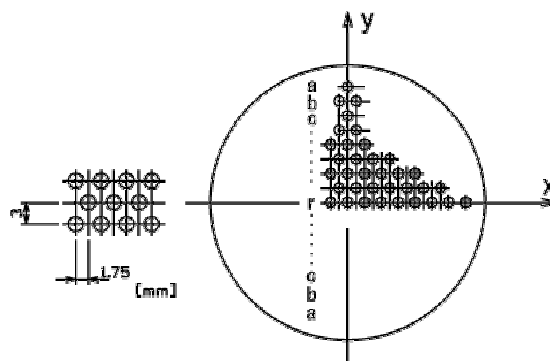


Figure 6. Schematic diagram of grid
Axis of x and y is defined this diagram. Axis of z is defined as the direction toward from this paper. And grid of upstream side is a plate of $z=0$.

1. Screen grid

Figure 7 shows close-view of screen grid holes. There is little characteristic shape change even if the position changes into radial direction on downstream side and up stream side. But, on upstream side, this grid surface is color like metal and slippery. It is considered the metal deposition by the sputtering in ionized chamber.

2. Accelerator grid

Figure 8 shows close-view of accelerator grid holes. Center grid hole r16 is a little larger than other grid holes on downstream side. On upstream side, most of grid hole have shape near the circle. Moreover, the mark of a diameter that is bigger than the accelerator grid was attached to both sides. It is because of decelerator grid or state of downstream plasma on downstream side. In the other hand, the marks on upstream is because of screen grid or state of ionized chamber.

3. Decelerator grid

Compared of other grids, screen and accelerator, decelerator grid holes abraded terribly. Seeing center grid hole r16, it abraded in a hexagonal shape on both sides. And it can be expected that the section shape has extended from the upstream to the downstream. Grid hole r7 which is position of about 3/4 of radius is a little erosion. It is considered that the ion is efficiently extracted from ionized chamber. However, grid hole r2 is asymmetry erosion on downstream side in contrast of other grid hole. There is metal deposition on both surface and it is rough.

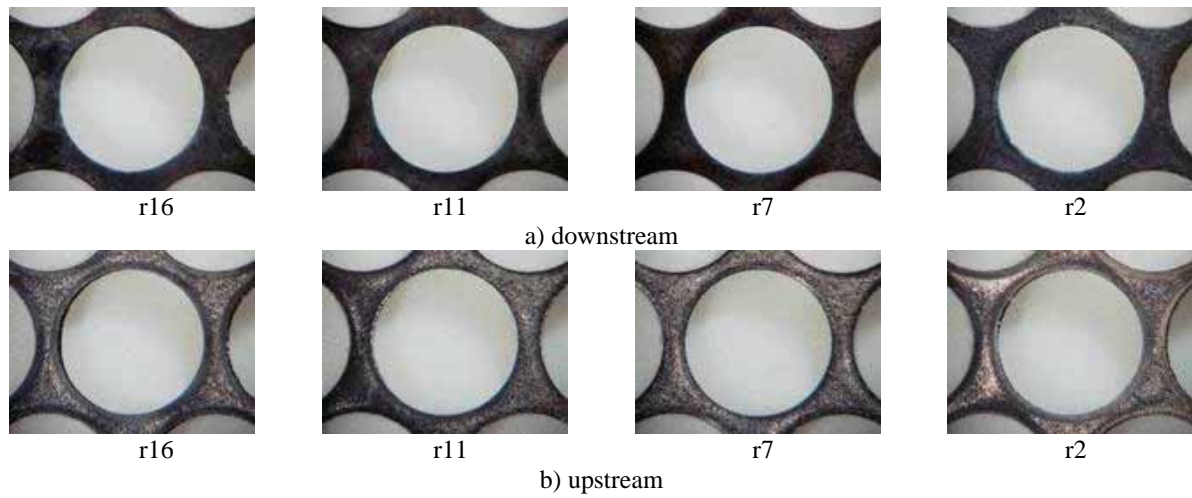


Figure 7. Close-up view of Screen grid hole after endurance test

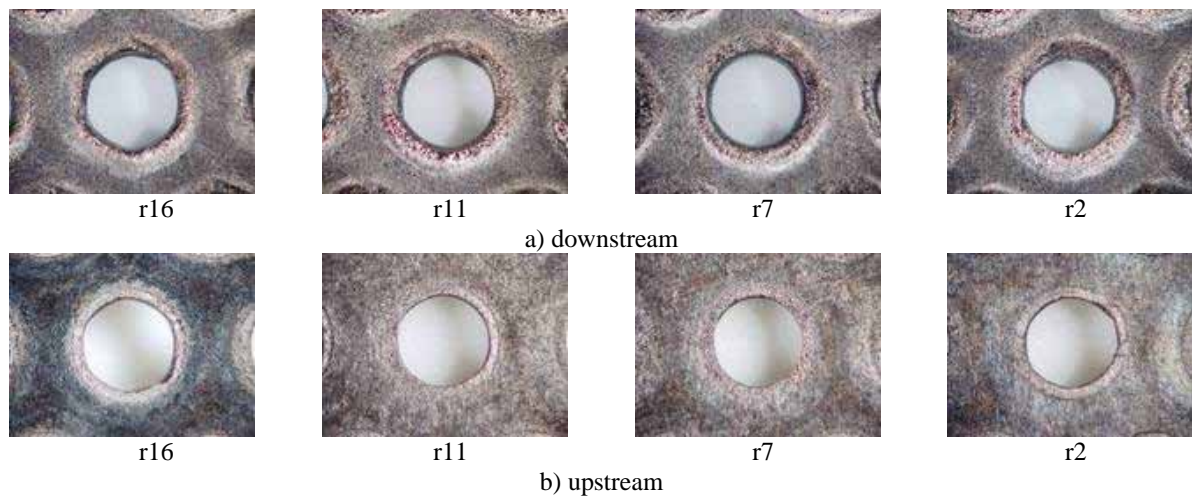


Figure 8. Close-up view of accelerator grid hole after endurance test

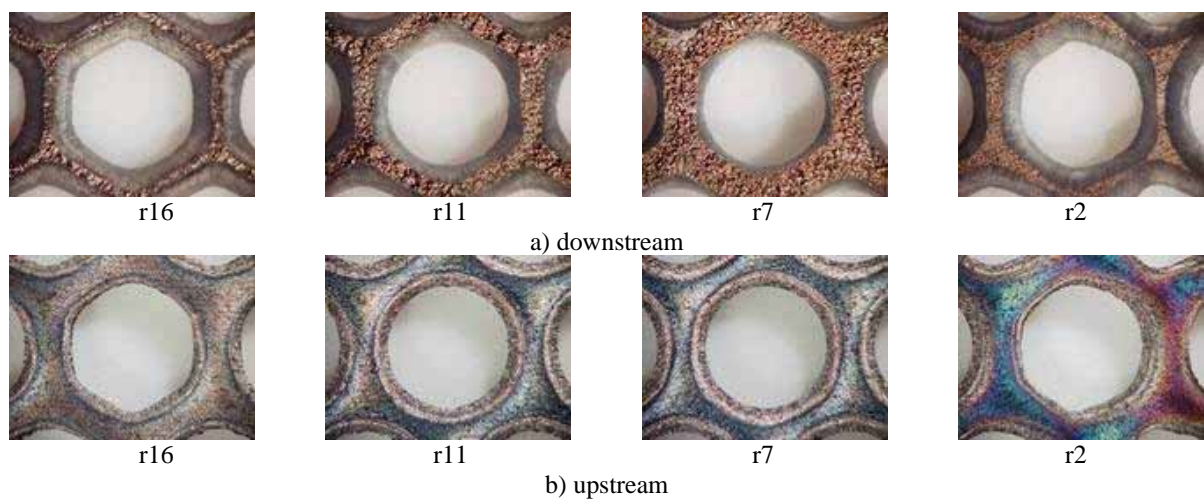


Figure 9. Close-up view of decelerator grid hole after endurance test

C. Measurement of Screen grid hole

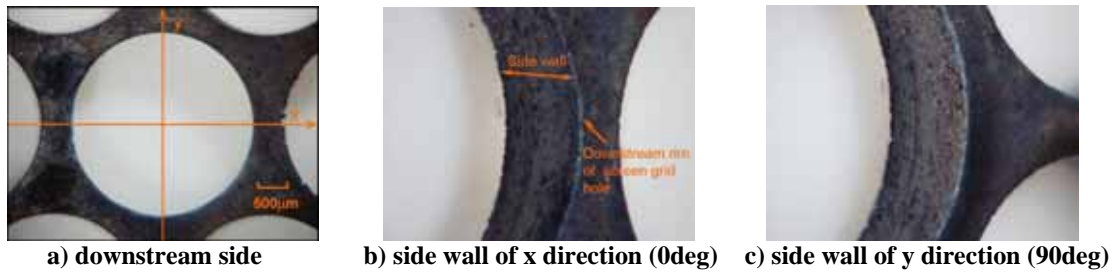


Figure 10. Close-up view of center hole of screen grid (position: r16). z axis is defined in the direction toward from space. b) and c) show side wall of screen grid when z axis is inclined to 45 degrees.

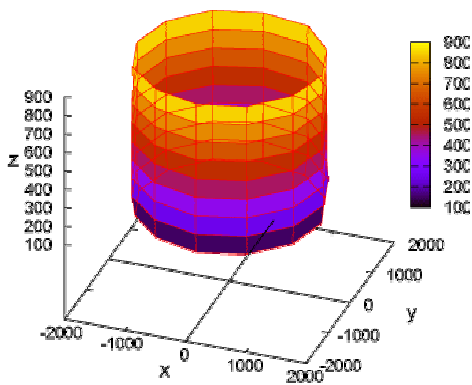


Figure 11. Shape of hole side wall on screen grid r16 (unit μm)

Downstream surface and upstream one are a plate of $z=0$ and plate of $z=1000$, respectively.

There is little metal deposition on side wall by close-up view Fig.10 b) and c). Figure 11 shows 3 dimensional shape of side wall every $z=100$ ($z=0$ is downstream surface before endurance test.). It made cross section shape characteristic like Fig. 12 and Radius characteristic like contour line (view of z direction).

Seeing Fig.12, we can understand that side wall of the height range $z=200$ to 800 is increased own diameter a little. In other words, this hole looks like barrel type. However, it considers that this erosion of screen grid hole is no problem to operate this ion engine and efficiently extract the ion from ionized chamber.

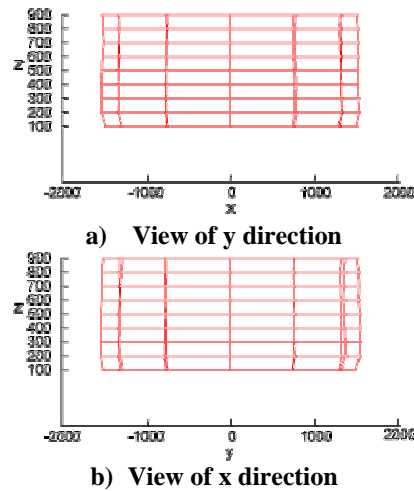


Figure 12. Cross section shape characteristic of screen grid hole r16 (unit μm)

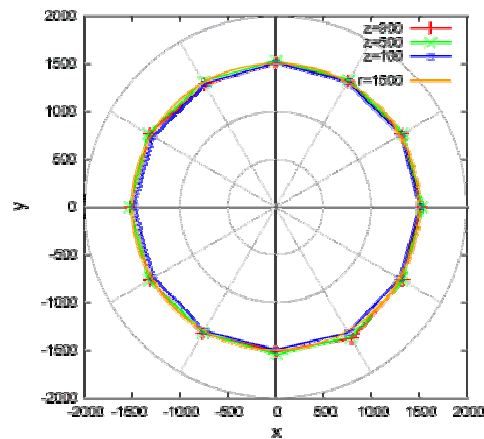


Figure 13. Radius characteristic of screen grid hole r16 (unit μm)

D. Accelerator grid



Figure 14. Close-up view of center hole of screen grid (position: r16). z axis is defined in the direction toward from space. *b*) and *c*) show side wall of screen grid when z axis is inclined to 45 degrees.

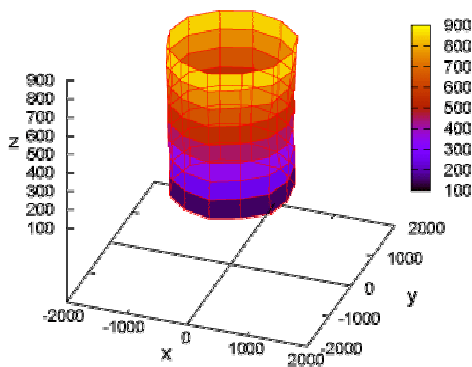


Figure 15. Shape of hole side wall on accelerator grid r16 (unit μm)
Downstream surface and upstream one are a plate of $z=0$ and plate of $z=1000$, respectively.

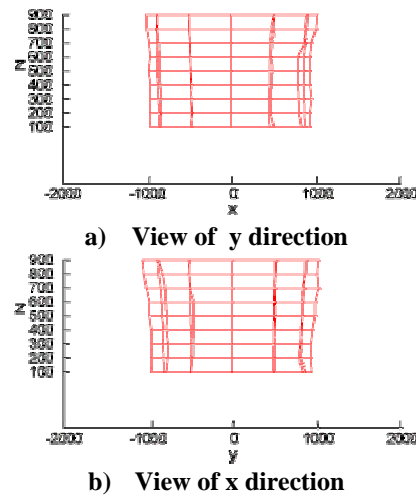


Figure 16. Cross section shape characteristic of accelerator grid hole r16 (unit μm)

There is a little metal deposition on downstream rim (Fig. 14). Figures 15 to 17 show as well as screen grid.

Seeing Fig. 16 and 17, we can understand that this erosion is symmetry at z axis. And this shape at view of z axis is a little hexagonal. Downstream rim is wider than own one before endure test and upstream rim is a little. And middle height (about $z=500$) have little erosion or a little metal deposition. This hole shape look like throat type.

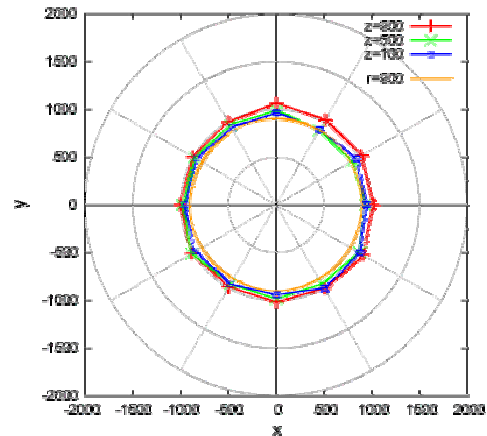


Figure 17. Radius characteristic of accelerator grid hole r16 (unit μm)

E. Decelerator grid



Figure 18. Close-up view of center hole of screen grid (position: r16). z axis is defined in the direction toward from space. *b)* and *c)* show side wall of screen grid when z axis is inclined to 45 degrees.

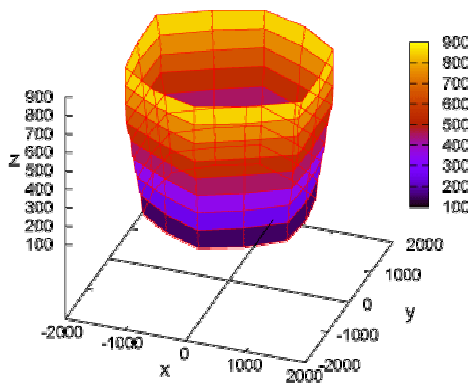


Figure 19. Shape of hole side wall on decelerator grid r16 (unit μm)
Downstream surface and upstream one are a plate of $z=0$ and plate of $z=1000$, respectively.

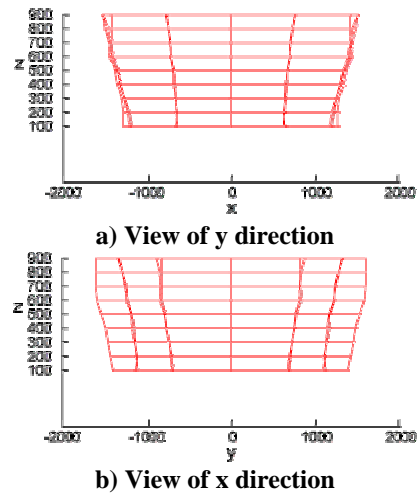


Figure 20. Cross section shape characteristic of decelerator grid hole r16 (unit μm)

To see Fig. 20, there is metal deposition, considered sputtering from downstream on downstream rim. This surface is very rough. Figures 19 to 21 show as well as screen grid.

In cross section shape characteristic, the wide of view of x direction is larger than y direction at downstream side $z=900$. The width of cross section x axis at $z=900$ is $3000\mu\text{m}$ at $z=900$. But this at $z=100$ is $2500\mu\text{m}$, which is diameter of decelerator grid hole. In the other hand, it is and this center grid hole r16 is abrades in a hexagonal shape (Fig.21.). it is considered that each grid hole is aligned and one grid hole shape after endurance test affect outcome of extracting ion from other grid hole.

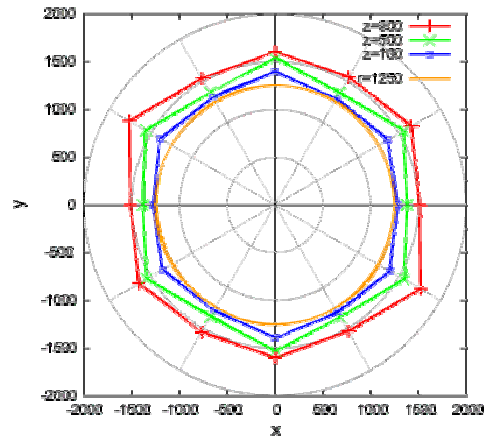


Figure 21. Radius characteristic of decelerator grid hole r16 (unit μm)

V. Conclusion

In this study, the following findings were obtained.

- Cross section shape characteristic and Radius characteristic of hole shape on C/C composite grid after 20,000-hour Endurance Test is understood.
- Erosion of screen grid hole is little.
- Shape of accelerator grid hole after endurance test is throat type.
- Shape of decelerator grid hole after endurance test is wider than other grids. And it looks like pot type (rim of downstream side is flare)
- Surface of accelerator grid and decelerator grid was very rough on both upstream side and downstreamside.
- We need to measure shape of grid surface.

Reference

- ¹Brophy, J. R., Polk, J. E., and Rawlin, V. K., "Ion Life Validation by Analysis and Testing," AIAA Paper 96-2715, July 1996.
- ²Hedges, D. E., and Meserole, J. E., "Demonstration and Evaluation of Carbon-Carbon Ion Optics," *Journal of Propulsion and Power*, Vol. 10, 1994, pp. 255-261.
- ³Meserole, J. E., "Measurement of Relative Erosion Rate of Carbon-Carbon and Molybdenum Optics," AIAA Paper 94-3119, June 1994.
- ⁴Meserole, J. E., Brophy, J. R., and Brown, D. k., "Performance Characteristics of 15-cm Carbon-Carbon Composite Grid," AIAA Paper 94-3118, June 1994.
- ⁵Muellor,J., Brown, D. K., Garner, C. E., and Brophy, J. R., "Fabrication of Carbon-Carbon Grids for Ion Optics," *Proceedings of the 23rd International Electric Propulsion Conference*, The Electric Rocket Propulsion Society, Seattle, 1993, pp. 1041-1049.
- ⁶Garner, G. E., and Brophy, J. R., "Fabrication and Testing of Carbon-Carbon Grid for Ion Optics," AIAA Paper 92-3149, July 1992.
- ⁷Kitamura, S., Hayakawa, Y., Kasai, Y., and Ozaki, T., "Fabrication of Carbon-Carbon Composite Ion Thruster Grids – Improvement of Structural Strength," *Proceedings of the 25th International Electric Propulsion Conference*, The Electric Rocket Propulsion Society, Cleveland, OH, 1997, 1997, pp. 586-593.
- ⁸Groh, K. H., Leiter, H. J., and Lob, H. W., "Design and Performance of the New RF-Ion Thruster RIT 15," AIAA Paper 98-3344, July 1998.
- ⁹Paterson, M. J., Domonkos, M. T., Foster, J. E., Hag, T. W., Manteniaks, M. A., Pinero, L. R., Sarver-Verhey, T.R., Soulas, G. C., Sovey, J.S., and Strzempkowski, E., "Ion Propulsion Development Activities at NASA Glenn Research Center," AIAA Paper 2000-3810,2000.
- ¹⁰Buckley, J. D., "Carbon-Carbon, An Overview," *Ceramic Bulletin*, Vol.67, No. 2, 1988, pp. 4228, 4229.
- ¹¹Metal Data Book, edited by Japan Inst. of Metals, Maruzen, Tokyo, 1984, p.35 (in Japanese).
- ¹²Meserole, J. E., "Measurement of Relative Erosion Rate of Carbon-Carbon and Molybdenum Optics," AIAA Paper 94-3119, June 1994.
- ¹³Funaki, I., Kuninaka, H., Toki, K., Shimizu, Y., Nishiyama, K., and Horiuchi, Y., "Verification Tests of Carbon-Carbon Composite Grids for Microwave Discharge Ion Thruster," *Journal of Propulsion and Power*, Vol. 18, 2002, pp. 169-175..
- ¹⁴Toki, K., Kuninaka, Y., Nishiyama, Shimizu, Y., "Flight Readiness of the Microwave Ion Engine System for MUSES-C Mission," *Proceedings of the 28th International Electric Propulsion Conference*, The Electric Rocket Propulsion Society, France, IEPC-2003-98.
- ¹⁵Meserole, J. S., and Hedges, D. E., "Comparison of Erosion Rates of Carbon-Carbon and Molybdenum Ion optics," *Proceedings of the 23rd International Electric Propulsion Conference*, The Electric Rocket Propulsion Society, Seattle, 1993, pp. 1032-1040.